DAFTAR PUSTAKA

Adysahwan;Syafri, & Syahriar Tato. (2022). Tipologi dan Perubahan Pemanfaatan Ruang. *Urban and Regional Studies Journal*, *4*(2), 94–101. https://doi.org/10.35965/ursj.v4i2.1464

Akher, S., & Chattopadhyay, D. S. (2017). Impact of Urbanization on Land Surface Temperature - A Case Study of Kolkata New Town. *The International Journal of Engineering and Science*, *6*(01), 71–81. https://doi.org/10.9790/1813-0601027181

Ar-Rahiem, M. M., Fakhlevi, M. R., & Hekmatyar, M. I. (2019). Analisis Fenomena Pulau Panas Perkotaan Kota Bandung Menggunakan Google Earth Engine. *Seminar Nasional Penginderaan Jauh Ke-6*, *September*, 61–68.

Arifin, D., Rahma, N. E., & Maharani, R. (2018). Identifikasi Tutupan Lahan Kota Samarinda Dengan Memanfaatkan Citra Satelit Landsat-8 Dan Algoritma Ndvi. *Elipsoida : Jurnal Geodesi Dan Geomatika*, *1*(02), 79–84. https://doi.org/10.14710/elipsoida.2018.3470

Arsy, R. F. (2010). Metode Survei Deskriptif untuk Mengkaji Kemampuan Interpretasi Citra pada Mahasiswa Pendidikan Geografi FKIP Universitas Tadulako. *Jurnal FKIP Universitas Tadulako*, 62–72.

Bakry, G. N. (2011). *Analisis Peningkatan Suhu Permukaan Akibat Konversi Lahan Dengan Menggunakan Citra Landsat Etm+ (Studi Kasus : Jakarta)*. Institut Pertanian Bogor.

Bereta, K., Koubarakis, M., Pantazi, D. A., Stamoulis, G., Caumont, H., Daniels, U., Dirk, D., Ubels, S., Venus, V., & Wahyudi, F. (2019). Providing Satellite Data to Mobile Developers Using Semantic Technologies and Linked Data. *Proceedings - 13th IEEE International Conference on Semantic Computing, ICSC 2019*, 348–351. https://doi.org/10.1109/ICOSC.2019.8665579

BPS (Badan Pusat Statistik). (2021). Berita Resmi Statistik No. 7/01/Th. XXIV, 21 Januari 2021. In *Bps.Go.Id*. https://papua.bps.go.id/pressrelease/2018/05/07/336/indeks-pembangunan-manusia-provinsi-papua-tahun-2017.html

BPS Sinjai. (2023). *Kabupaten Sinjai Dalam Angka 2023*.

BSN. (2014). SNI 7645-1:2014 Klasifikasi penutup lahan - Bagian 1 : Skala kecil dan menengah. In *Sni* (Vols. 7645–1). https://kupdf.net/downloadFile/59edda7908bbc53933eb8a1f

Cohen, J. (1968). Weighted kappa: Nominal scale agreement provision for scaled disagreement or partial credit. *Psychological Bulletin*, *70*(4), 213–220. https://doi.org/10.1037/h0026256

Delarizka, A., Sasmito, B., & Hani'ah. (2016). Analisis Fenomena Pulau Bahang (Urban Heat Island) Di Kota Semarang Berdasarkan Hubungan Antara Perubahan Tutupan Lahan Dengan Suhu Permukaan Menggunakan Citra Multi Temporal Landsat. *Jurnal Geodesi Undip*, *5*, 165–175.

Dong, J., Xiao, X., Menarguez, M. A., Zhang, G., Qin, Y., Thau, D., Biradar, C., & Moore, B. (2016). Mapping paddy rice planting area in northeastern Asia with Landsat 8 images, phenology-based algorithm and Google Earth Engine. *Remote Sensing of Environment*, *185*, 142–154. https://doi.org/10.1016/j.rse.2016.02.016

Du, C., Ren, H., Qin, Q., Meng, J., & Zhao, S. (2015). A practical split-window algorithm for estimating land surface temperature from landsat 8 data. *Remote Sensing*, *7*(1), 647–665. https://doi.org/10.3390/rs70100647

Dwisyahputra, I, R. (2023). *Hubungan kerapatan vegetasi dengan suhu permukaan tanah di kota balikpapan*.

Filchev, L., Pashova, L., Kolev, V., & Frye, S. (2018). Challenges and Solutions for Utilizing Earth Observations in the "Big Data" Era. *BigSkyEarth Conference: AstroGeoInformatics, Tenerife, Spain, December 17-19, 2018*, 1–6.

Gorelick, N., Hancher, M., Dixon, M., Ilyushchenko, S., Thau, D., & Moore, R. (2017). Google Earth Engine: Planetary-scale geospatial analysis for everyone. *Remote Sensing of Environment*, *202*, 18–27. https://doi.org/10.1016/j.rse.2017.06.031

Guntara, I. (2015). Pemanfaatan Citra Landsat 8 untuk Mengestimasi Suhu Permukaan Lahan (Land Surface Temperature) di Kabupaten Bantul Menggunakan Split Window Algorithm. In *Universitas Gadjah Mada*. Universitas Gadjah Mada.

Handayani, D., & Setiyadi, A. (2003). Remote Sensing [Penginderaan Jauh]. *Edisi Mei*, *7*(2), 113–120.

Handayani, N. (2007). Identifikasi Perubahan Kapasitas Panas Kawasan Perkotaan Dengan Menggunakan Citra Landsat Tm/Etm+ (Studi Kasus : Kodya Bogor). *Skripsi*.

Handoko. (1995). *Klimatologi Dasar*. Pustaka Jaya.

Holmes, T. R. H., Hain, C. R., Anderson, M. C., & Crow, W. T. (2016). Cloud tolerance of remote-sensing technologies to measure land surface temperature. *Hydrology and Earth System Sciences*, *20*(8), 3263–3275. https://doi.org/10.5194/hess-20-3263-2016

Hu, W., Zhou, W., & He, H. (2015). The effect of land-use intensity on surface temperature in the dongting lake area, China. *Advances in Meteorology*, *2015*. https://doi.org/10.1155/2015/632151

IPCC. (2014). *Climate Change 2014: Mitigation of Climate Change* (Vol. 38, Issue 2). https://doi.org/10.2134/jeq2008.0024br

Kalfuadi, Y. (2009). Analisis Temperature Heat Index (THI) Dalam Hubungannya Dengan Ruang Terbuka Hijau. (Studi Kasus : Kabupaten Bungo - Propinsi Jambi). *Meteorologi IPB*, 27.

Karina, R. K., & Kurniawan, R. (2021). Identifikasi Penggunaan Lahan Menggunakan Citra Satelit Landsat 8 Melalui Google Earth Engine. *Seminar Nasional Official Statistics*, *2020*(1), 798–805.

https://doi.org/10.34123/semnasoffstat.v2020i1.514

Kehutanan, K. L. H. dan. (2015). Peraturan Direktur Jenderal dan Planologi Kehutanan nomor: P.1/VII-IPSDH/2015 Tentang Pedoman Pemantauan Penutupan Lahan. In *Kementerian Lingkungan Hidup dan Kehutanan Direktorat Jenderal Planologi Kehutanan* (pp. 1–17).

Khalil, B. (2016). Arahan Pengembangan Ruang Terbuka Hijau Berdasarkan Distribusi Suhu Permukaan Di Kawasan Metropolitan Mamminasata. Universitas Hasanuddin.

Komarudin, R. (2017). *Pedoman Pengolahan Data Penginderaan Jauh Landsat 8 untuk MPT*.

Kuenzer, C., & Dech, S. (2013). Thermal remote sensing Sensors, Methods, Applications. *Remote Sensing and Digital Image Processing*, *17*(July 2013), 287–313. https://doi.org/10.1007/978-94-007-6639-6

Lillesand, T., Kiefer, R. W., & Chipman, J. (2004). Remote Sensing and Image Interpretation. (John Wiley and Sons, Ed.). *The Geographical Journal*, *146*(3), 448–449.

Marlina, D. (2022). Klasifikasi Tutupan Lahan pada Citra Sentinel-2 Kabupaten Kuningan dengan NDVI dan Algoritme Random Forest. *STRING (Satuan Tulisan Riset Dan Inovasi Teknologi)*, *7*(1), 41. https://doi.org/10.30998/string.v7i1.12948

Mateo-García, G., Gómez-Chova, L., Amorós-López, J., Muñoz-Marí, J., & Camps-Valls, G. (2018). Multitemporal cloud masking in the Google Earth Engine. *Remote Sensing*, *10*(7), 7–9. https://doi.org/10.3390/rs10071079

Myint, S. W., Wentz, E. A., Brazel, A. J., & Quattrochi, D. A. (2013). The impact of distinct anthropogenic and vegetation features on urban warming. *Landscape Ecology*, *28*(5), 959–978. https://doi.org/10.1007/s10980-013-9868-y

Pradana, B., Ariani, N. M., & Pugara, A. (2020). *Pengaruh Penggunaan Lahan Terhadap Suhu*. *4*(2), 92–100.

Prasasti, I., Ari Sambodo, K., & Carolita, I. (2007). Pengkajian Pemanfaatan Data TERRA-MODIS Untuk Ekstraksi Data Suhu Permukaan Lahan (SPL) Berdasarkan Beberapa Algoritma (The Study of Application of TERRA-MODIS for Land Surface Temperature Extraction Based on Several Algorithms). *Jurnal Penginderaan Jauh*, *4*(1), 1–8. www.modis.gsfc.

Prayogo, L. M. (2021). Platform Google Earth Engine Untuk Pemetaan Suhu Permukaan Daratan Dari Data Series Modis. *Journal of Computer and Information Technology*, *5*(1), 25. https://doi.org/10.25273/doubleclick.v5i1.8604

Safitri, R., Vonnisa, M., & Marzuki, M. (2022). Analisis Dampak Perubahan Tutupan Lahan di Kalimantan Terhadap Temperatur Permukaan. *Jurnal Fisika Unand*, *11*(2), 173–179. https://doi.org/10.25077/jfu.11.2.173-179.2022

Sampurno, R., & Thoriq, A. (2016). Klasifikasi Tutupan Lahan Menggunakan Citra Landsat 8 Operational Land Imager (Oli) Di Kabupaten Sumedang. *Jurnal*

Teknotan, *10*(2), 61–70. https://doi.org/10.24198/jt.vol10n2.9

Sejati, A. W., Buchori, I., & Rudiarto, I. (2019). The spatio-temporal trends of urban growth and surface urban heat islands over two decades in the Semarang Metropolitan Region. *Sustainable Cities and Society*, *46*(January), 101432. https://doi.org/10.1016/j.scs.2019.101432

Susandi, A., Herlianti, I., Tamamadin, M., & Nurlela, I. (2010). Dampak Perubahan Iklim Terhadap Ketinggian Muka Laut Di Wilayah Banjarmasin. *Jurnal Ekonomi Lingkungan*, *12*(2), 5–8.

Tamiminia, H., Salehi, B., Mahdianpari, M., Quackenbush, L., Adeli, S., & Brisco, B. (2020). Google Earth Engine for geo-big data applications: A meta-analysis and systematic review. *ISPRS Journal of Photogrammetry and Remote Sensing*, *164*(January), 152–170. https://doi.org/10.1016/j.isprsjprs.2020.04.001

Tosiani, A. (2020). *Akurasi Data Penutupan Lahan Nasional Tahun 1990-2016*. 1–41.

U.S. Geological Survey. (2019). Landsat 8 Data Users Handbook. In *Sioux Falls: Department of the Interior U.S. Geological Survey*. https://landsat.usgs.gov/documents/Landsat8DataUsersHandbook.pdf

USGS. (2022). *Landsat 8-9 Level 2 Science Product (L2SP) Guide March 2022 Landsat 8-9*. *2*(March).

Utomo, A. W., Suprayogi, A., & Sasmito, B. (2015). Analisis Hubungan Variasi Land Surface Temperature Dengan Kelas Tutupan Lahan Menggunakan Data Citra Satelit Landsat (Studi Kasus : Kabupaten Pati). *Jurnal Geodesi Undip*, *4*(April), 86–94.

Wiweka. (2014). *Satelit Landsat Multitemporal E Surface and Air Temperature Pattern Using*. 11–22.

Yollanda, A. (2011). Kajian Perubahan Penutup Lahan Dengan Menggunakan Teknik Penginderaan Jauh Multi-Temporal Di Daerah Aliran Sungai Bodri. *Jurusan Geografi*.

Yusuf, D., & Rijal, S. A. S. (2001). Buku Ajar Penginderaan Jauh Program Studi Pendidkan Geografi. In *Program Studi Pendidikan Geografi*.

Zhang, T., Su, J., Xu, Z., Luo, Y., & Li, J. (2021). Sentinel-2 satellite imagery for urban land cover classification by optimized random forest classifier. *Applied Sciences (Switzerland)*, *11*(2), 1–17. https://doi.org/10.3390/app11020543

LAMPIRAN

Lampiran 1. Daerah Latih Penutupan Lahan Tahun 2015 dan 2023

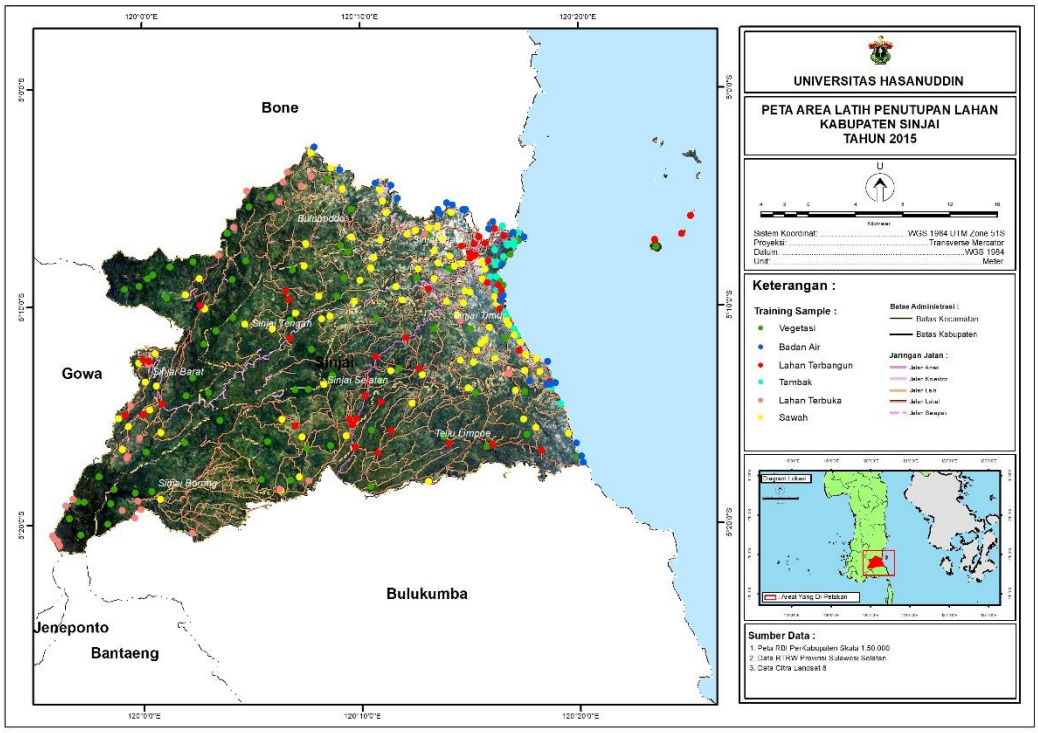

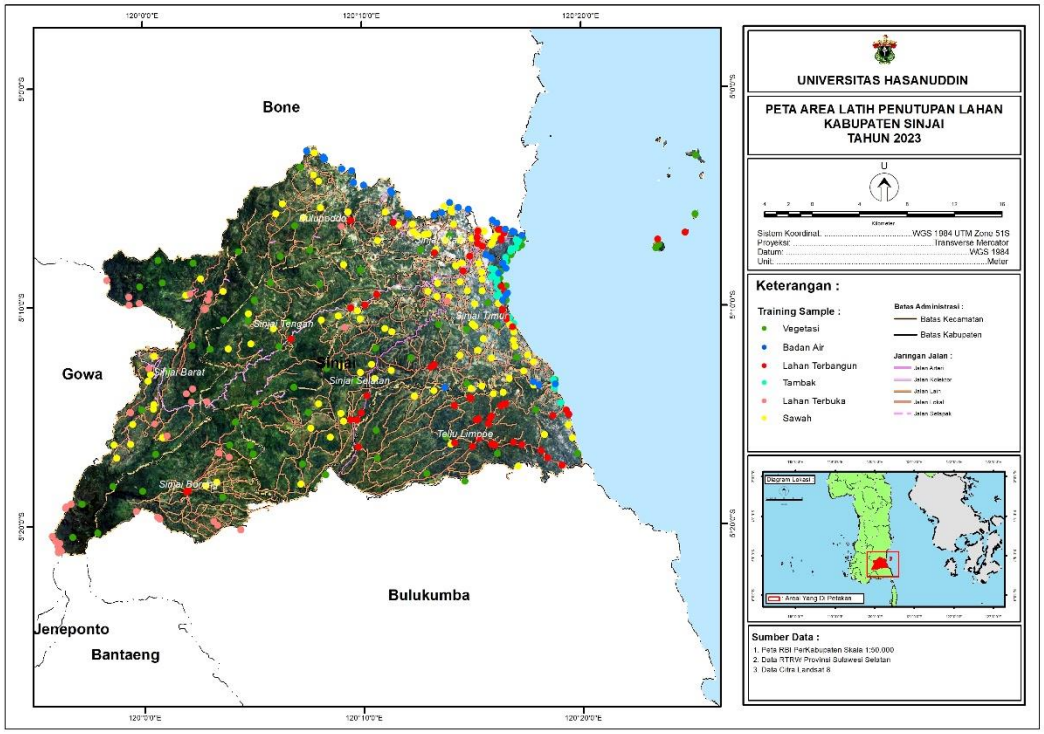

Lampiran 2. Perbandingan kondisi tipe penutupan lahan

No	Kelas Penutupan Lahan	Kondisi Lapangan 2021	Kenampakan Citra Landsat 8 Kombinasi Band 654
1	Vegetasi		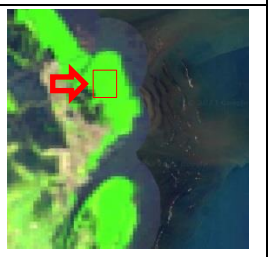
2	Badan Air		
3	Lahan Terbangun		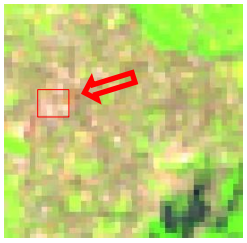
4	Tambak		
5	Lahan Terbuka		

No	Kelas Penutupan Lahan	Kondisi Lapangan 2021	Kenampakan Citra Landsat 8 Kombinasi Band 654
6	Sawah		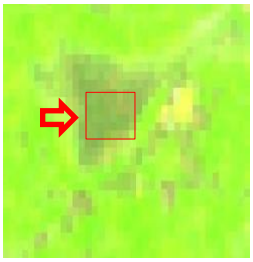
7	Vegetasi		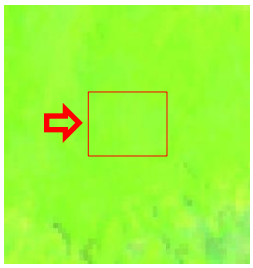
8	Lahan Terbangun		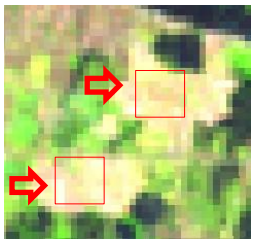
9	Badan Air	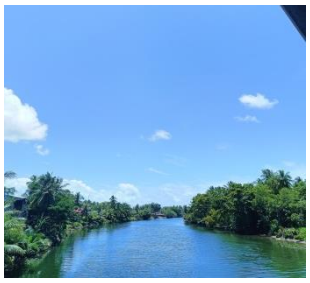	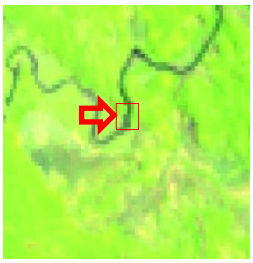
10	Sawah		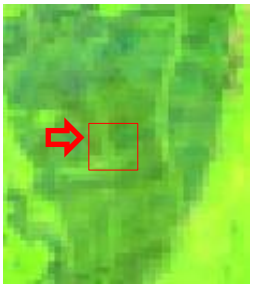

Lampiran 3. Hasil Pengecekan Lapangan Tahun 2023

Titik	Kelas Penutupan Lahan	Kesesuaian	Perubahan	Koordinat (UTM)	
				X	Y
1	Vegetasi	Sesuai		199204.57	9433872.61
2	Lahan Terbangun	Sesuai		198665.88	9434035.59
3	Tambak	Sesuai		198165.36	9433959.40
4	Lahan Terbangun	Sesuai		197933.84	9434250.45
5	Vegetasi	Sesuai		196239.11	9432741.98
6	Vegetasi	Sesuai		194999.63	9434558.66
7	Badan Air	Sesuai		198796.59	9434369.18
8	Lahan Terbangun	Sesuai		195166.63	9432252.42
9	Badan Air	Sesuai		195962.96	9432646.32
10	Badan Air	Sesuai		195105.31	9431712.73
11	Vegetasi	Sesuai		193651.95	9432687.46
12	Vegetasi	Sesuai		191129.87	9434015.97
13	Sawah	Sesuai		191085.95	9431394.26
14	Sawah	Sesuai		194636.40	9428837.72
15	Tambak	Sesuai		196884.04	9431089.33
16	Tambak	Sesuai		197373.52	9429687.03
17	Vegetasi	Sesuai		197984.71	9428678.31
18	Vegetasi	Sesuai		197548.15	9430361.72
19	Tambak	Sesuai		196992.52	9432107.97
20	Tambak	Sesuai		197806.12	9432994.33
21	Tambak	Sesuai		198321.66	9427381.77
22	Badan Air	Sesuai		196229.92	9427202.51
23	Badan Air	Tidak Sesuai	Tambak	201798.09	9421626.27
24	Lahan Terbangun	Sesuai		201882.28	9421829.53
25	Vegetasi	Tidak Sesuai	Sawah	200857.11	9421053.41
26	Vegetasi	Sesuai		182883.30	9428705.64
27	Lahan Terbuka	Sesuai		175048.97	9425482.30
28	Lahan Terbuka	Tidak Sesuai	Vegetasi	173981.11	9428785.90
29	Lahan Terbuka	Sesuai		167654.06	9419609.97
30	Lahan Terbangun	Sesuai		169083.70	9419974.39
31	Lahan Terbuka	Tidak Sesuai	Sawah	166509.30	9419952.69
32	Lahan Terbangun	Sesuai		165753.65	9418933.52
33	Sawah	Sesuai		166393.41	9416473.62
34	Sawah	Sesuai		169032.63	9417161.53
35	Vegetasi	Sesuai		165315.23	9414595.07
36	Vegetasi	Sesuai		164971.27	9416731.58
37	Vegetasi	Sesuai		171035.12	9416266.74
38	Sawah	Sesuai		172440.25	9411208.06
39	Lahan Terbuka	Sesuai		172315.15	9410543.22

Titik	Kelas Penutupan Lahan	Kesesuaian	Perubahan	Koordinat (UTM)	
				X	Y
40	Vegetasi	Sesuai		170317.54	9409815.61
41	Vegetasi	Sesuai		168227.33	9411284.05
42	Sawah	Sesuai		180880.66	9413136.40
43	Lahan Terbangun	Sesuai		202020.91	9415251.75
44	Vegetasi	Sesuai		201997.10	9415058.60
45	Lahan Terbangun	Sesuai		202663.85	9414816.51
46	Lahan Terbangun	Sesuai		204395.68	9414904.62
47	Badan Air	Sesuai		204443.31	9414813.71
48	Tambak	Sesuai		198811.11	9426255.11
49	Tambak	Sesuai		199160.36	9425479.87
50	Lahan Terbangun	Sesuai		197765.76	9429384.81
51	Lahan Terbangun	Sesuai		184470.80	9435437.94
52	Sawah	Tidak Sesuai	Vegetasi	184183.99	9435409.37
53	Sawah	Sesuai		183893.88	9437149.34
54	Lahan Terbangun	Sesuai		183292.91	9439229.84
55	Sawah	Sesuai		183549.03	9439183.27
56	Lahan Terbangun	Sesuai		181768.80	9439908.07
57	Vegetasi	Sesuai		179801.29	9437158.65
58	Vegetasi	Sesuai		176446.63	9435695.94
59	Vegetasi	Tidak Sesuai	Sawah	191154.57	9415693.60
60	Lahan Terbangun	Sesuai		193315.69	9416611.44
61	Sawah	Sesuai		192200.21	9413836.91
62	Vegetasi	Sesuai		190260.28	9421427.37
63	Sawah	Sesuai		184241.73	9420755.95
64	Sawah	Sesuai		185954.91	9420008.50
65	Sawah	Sesuai		186767.18	9423130.06
66	Vegetasi	Sesuai		168284.67	9412354.06
67	Vegetasi	Sesuai		191542.33	9426628.02
68	Sawah	Sesuai		189788.63	9428689.93
69	Vegetasi	Sesuai		169168.36	9428336.51
70	Vegetasi	Sesuai		171538.36	9431576.51
71	Vegetasi	Sesuai		175276.90	9433046.25
72	Sawah	Tidak Sesuai	Vegetasi	177462.96	9435691.36
73	Lahan Terbuka	Tidak Sesuai	Sawah	172670.02	9417801.51
74	Sawah	Sesuai		167999.06	9422698.43
75	Vegetasi	Sesuai		169618.31	9423301.68
76	Lahan Terbangun	Sesuai		167815.00	9423407.81
77	Sawah	Sesuai		168015.82	9423875.07
78	Vegetasi	Sesuai		172388.63	9426799.93
79	Vegetasi	Sesuai		200108.63	9416779.93
80	Tambak	Sesuai		202714.94	9420048.22

Titik	Kelas Penutupan Lahan	Kesesuaian	Perubahan	Koordinat (UTM)	
				X	Y
81	Vegetasi	Sesuai		198883.54	9422019.59
82	Vegetasi	Sesuai		188489.37	9430273.22
83	Sawah	Sesuai		193333.90	9428521.68
84	Sawah	Sesuai		186588.99	9431449.30
85	Lahan Terbangun	Sesuai		195547.69	9433499.84
86	Sawah	Sesuai		194749.20	9429963.77
87	Vegetasi	Sesuai		188782.33	9434998.02
88	Vegetasi	Sesuai		184565.37	9436448.46
89	Vegetasi	Sesuai		197843.14	9416183.49
90	Vegetasi	Sesuai		182956.94	9424128.46
91	Vegetasi	Sesuai		183718.94	9429166.13
92	Vegetasi	Sesuai		171275.56	9425035.98
93	Sawah	Sesuai		171294.58	9428818.61
94	Vegetasi	Sesuai		177797.05	9430564.93
95	Sawah	Sesuai		195699.80	9431098.00
96	Tambak	Sesuai		197542.41	9433652.95
97	Lahan Terbangun	Sesuai		195588.29	9434565.93
98	Sawah	Sesuai		194450.58	9433047.22
99	Vegetasi	Sesuai		194302.41	9432703.26
100	Vegetasi	Sesuai		193360.67	9431713.54

Lampiran 4. Kappa Accuracy Penutupan Lahan Tahun 2023

Kelas Penutupan Lahan		Hasil Pengecekan Lapangan						Total
		Vegetasi	Badan Air	Lahan Terbangun	Tambak	Lahan Terbuka	Sawah	
Hasil Interpretasi Tahun 2023	Vegetasi	36					2	38
	Badan Air		5		1			6
	Lahan Terbangun			17				17
	Tambak				10			10
	Lahan Terbuka	1				3	2	6
	Sawah	2					21	23
Total		39	5	17	11	3	25	100

Keterangan:

= Titik pengecekan lapangan yang sesuai dengan hasil interpretasi citra.

Kappa Accuracy =

$$Kappa\ (k) = \frac{N\ \Sigma\ X_n\ -\ \Sigma\ X_{n+}\ X_{+n}}{N^2\ -\ \Sigma\ X_{n+}X_{+n}} \times 100$$

= 89,33%

Lampiran 5. Koleksi Citra Yang digunakan dalam Analisis

Koleksi citra untuk melihat penutupan lahan.

Tahun 2015:

0: Image LANDSAT/LC08/C02/T1_L2/LC08_113064_20150410
1: Image LANDSAT/LC08/C02/T1_L2/LC08_113064_20150426
2: Image LANDSAT/LC08/C02/T1_L2/LC08_113064_20150512
3: Image LANDSAT/LC08/C02/T1_L2/LC08_113064_20150528
4: Image LANDSAT/LC08/C02/T1_L2/LC08_113064_20150613
5: Image LANDSAT/LC08/C02/T1_L2/LC08_113064_20150629
6: Image LANDSAT/LC08/C02/T1_L2/LC08_113064_20150715
7: Image LANDSAT/LC08/C02/T1_L2/LC08_113064_20150917
8: Image LANDSAT/LC08/C02/T1_L2/LC08_113064_20151003
9: Image LANDSAT/LC08/C02/T1_L2/LC08_114063_20150111
10: Image LANDSAT/LC08/C02/T1_L2/LC08_114063_20150127
11: Image LANDSAT/LC08/C02/T1_L2/LC08_114063_20150212
12: Image LANDSAT/LC08/C02/T1_L2/LC08_114063_20150228
13: Image LANDSAT/LC08/C02/T1_L2/LC08_114063_20150316
14: Image LANDSAT/LC08/C02/T1_L2/LC08_114063_20150401
15: Image LANDSAT/LC08/C02/T1_L2/LC08_114063_20150417
16: Image LANDSAT/LC08/C02/T1_L2/LC08_114063_20150503
17: Image LANDSAT/LC08/C02/T1_L2/LC08_114063_20150519
18: Image LANDSAT/LC08/C02/T1_L2/LC08_114063_20150604
19: Image LANDSAT/LC08/C02/T1_L2/LC08_114063_20150620
20: Image LANDSAT/LC08/C02/T1_L2/LC08_114063_20150706
21: Image LANDSAT/LC08/C02/T1_L2/LC08_114063_20150722
22: Image LANDSAT/LC08/C02/T1_L2/LC08_114063_20150807
23: Image LANDSAT/LC08/C02/T1_L2/LC08_114063_20150823
24: Image LANDSAT/LC08/C02/T1_L2/LC08_114063_20150908
25: Image LANDSAT/LC08/C02/T1_L2/LC08_114063_20150924
26: Image LANDSAT/LC08/C02/T1_L2/LC08_114063_20151010
27: Image LANDSAT/LC08/C02/T1_L2/LC08_114063_20151026
28: Image LANDSAT/LC08/C02/T1_L2/LC08_114063_20151111

29: Image LANDSAT/LC08/C02/T1_L2/LC08_114063_20151127
30: Image LANDSAT/LC08/C02/T1_L2/LC08_114063_20151213
31: Image LANDSAT/LC08/C02/T1_L2/LC08_114063_20151229
32: Image LANDSAT/LC08/C02/T1_L2/LC08_114064_20150111
33: Image LANDSAT/LC08/C02/T1_L2/LC08_114064_20150127
34: Image LANDSAT/LC08/C02/T1_L2/LC08_114064_20150212
35: Image LANDSAT/LC08/C02/T1_L2/LC08_114064_20150228
36: Image LANDSAT/LC08/C02/T1_L2/LC08_114064_20150316
37: Image LANDSAT/LC08/C02/T1_L2/LC08_114064_20150401
38: Image LANDSAT/LC08/C02/T1_L2/LC08_114064_20150503
39: Image LANDSAT/LC08/C02/T1_L2/LC08_114064_20150519
40: Image LANDSAT/LC08/C02/T1_L2/LC08_114064_20150604
41: Image LANDSAT/LC08/C02/T1_L2/LC08_114064_20150620
42: Image LANDSAT/LC08/C02/T1_L2/LC08_114064_20150706
43: Image LANDSAT/LC08/C02/T1_L2/LC08_114064_20150722
44: Image LANDSAT/LC08/C02/T1_L2/LC08_114064_20150807
45: Image LANDSAT/LC08/C02/T1_L2/LC08_114064_20150823
46: Image LANDSAT/LC08/C02/T1_L2/LC08_114064_20150908
47: Image LANDSAT/LC08/C02/T1_L2/LC08_114064_20150924
48: Image LANDSAT/LC08/C02/T1_L2/LC08_114064_20151010
49: Image LANDSAT/LC08/C02/T1_L2/LC08_114064_20151026
50: Image LANDSAT/LC08/C02/T1_L2/LC08_114064_20151111
51: Image LANDSAT/LC08/C02/T1_L2/LC08_114064_20151127
52: Image LANDSAT/LC08/C02/T1_L2/LC08_114064_20151213
53: Image LANDSAT/LC08/C02/T1_L2/LC08_114064_20151229

Tahun 2023:

0: Image LANDSAT/LC08/C02/T1_L2/LC08_113064_20220803
1: Image LANDSAT/LC08/C02/T1_L2/LC08_113064_20220819
2: Image LANDSAT/LC08/C02/T1_L2/LC08_113064_20220904
3: Image LANDSAT/LC08/C02/T1_L2/LC08_113064_20220920
4: Image LANDSAT/LC08/C02/T1_L2/LC08_113064_20221006
5: Image LANDSAT/LC08/C02/T1_L2/LC08_113064_20221022

6: Image LANDSAT/LC08/C02/T1_L2/LC08_113064_20221209
7: Image LANDSAT/LC08/C02/T1_L2/LC08_113064_20230126
8: Image LANDSAT/LC08/C02/T1_L2/LC08_113064_20230211
9: Image LANDSAT/LC08/C02/T1_L2/LC08_113064_20230315
10: Image LANDSAT/LC08/C02/T1_L2/LC08_113064_20230502
11: Image LANDSAT/LC08/C02/T1_L2/LC08_113064_20230518
12: Image LANDSAT/LC08/C02/T1_L2/LC08_113064_20230705
13: Image LANDSAT/LC08/C02/T1_L2/LC08_113064_20230806
14: Image LANDSAT/LC08/C02/T1_L2/LC08_113064_20230822
15: Image LANDSAT/LC08/C02/T1_L2/LC08_113064_20231009
16: Image LANDSAT/LC08/C02/T1_L2/LC08_113064_20231025
17: Image LANDSAT/LC08/C02/T1_L2/LC08_113064_20231126
18: Image LANDSAT/LC08/C02/T1_L2/LC08_114063_20220810
19: Image LANDSAT/LC08/C02/T1_L2/LC08_114063_20220826
20: Image LANDSAT/LC08/C02/T1_L2/LC08_114063_20220911
21: Image LANDSAT/LC08/C02/T1_L2/LC08_114063_20220927
22: Image LANDSAT/LC08/C02/T1_L2/LC08_114063_20221013
23: Image LANDSAT/LC08/C02/T1_L2/LC08_114063_20221029
24: Image LANDSAT/LC08/C02/T1_L2/LC08_114063_20221114
25: Image LANDSAT/LC08/C02/T1_L2/LC08_114063_20221130
26: Image LANDSAT/LC08/C02/T1_L2/LC08_114063_20221216
27: Image LANDSAT/LC08/C02/T1_L2/LC08_114063_20230101
28: Image LANDSAT/LC08/C02/T1_L2/LC08_114063_20230117
29: Image LANDSAT/LC08/C02/T1_L2/LC08_114063_20230202
30: Image LANDSAT/LC08/C02/T1_L2/LC08_114063_20230306
31: Image LANDSAT/LC08/C02/T1_L2/LC08_114063_20230322
32: Image LANDSAT/LC08/C02/T1_L2/LC08_114063_20230407
33: Image LANDSAT/LC08/C02/T1_L2/LC08_114063_20230525
34: Image LANDSAT/LC08/C02/T1_L2/LC08_114063_20230610
35: Image LANDSAT/LC08/C02/T1_L2/LC08_114063_20230626
36: Image LANDSAT/LC08/C02/T1_L2/LC08_114063_20230712
37: Image LANDSAT/LC08/C02/T1_L2/LC08_114063_20230728

38: Image LANDSAT/LC08/C02/T1_L2/LC08_114063_20230813
39: Image LANDSAT/LC08/C02/T1_L2/LC08_114063_20230829
40: Image LANDSAT/LC08/C02/T1_L2/LC08_114063_20230914
41: Image LANDSAT/LC08/C02/T1_L2/LC08_114063_20230930
42: Image LANDSAT/LC08/C02/T1_L2/LC08_114063_20231016
43: Image LANDSAT/LC08/C02/T1_L2/LC08_114063_20231101
44: Image LANDSAT/LC08/C02/T1_L2/LC08_114063_20231117
45: Image LANDSAT/LC08/C02/T1_L2/LC08_114064_20220810
46: Image LANDSAT/LC08/C02/T1_L2/LC08_114064_20220826
47: Image LANDSAT/LC08/C02/T1_L2/LC08_114064_20220911
48: Image LANDSAT/LC08/C02/T1_L2/LC08_114064_20220927
49: Image LANDSAT/LC08/C02/T1_L2/LC08_114064_20221013
50: Image LANDSAT/LC08/C02/T1_L2/LC08_114064_20221029
51: Image LANDSAT/LC08/C02/T1_L2/LC08_114064_20221114
52: Image LANDSAT/LC08/C02/T1_L2/LC08_114064_20221130
53: Image LANDSAT/LC08/C02/T1_L2/LC08_114064_20230101
54: Image LANDSAT/LC08/C02/T1_L2/LC08_114064_20230117
55: Image LANDSAT/LC08/C02/T1_L2/LC08_114064_20230322
56: Image LANDSAT/LC08/C02/T1_L2/LC08_114064_20230407
57: Image LANDSAT/LC08/C02/T1_L2/LC08_114064_20230509
58: Image LANDSAT/LC08/C02/T1_L2/LC08_114064_20230525
59: Image LANDSAT/LC08/C02/T1_L2/LC08_114064_20230610
60: Image LANDSAT/LC08/C02/T1_L2/LC08_114064_20230626
61: Image LANDSAT/LC08/C02/T1_L2/LC08_114064_20230712
62: Image LANDSAT/LC08/C02/T1_L2/LC08_114064_20230728
63: Image LANDSAT/LC08/C02/T1_L2/LC08_114064_20230813
64: Image LANDSAT/LC08/C02/T1_L2/LC08_114064_20230829
65: Image LANDSAT/LC08/C02/T1_L2/LC08_114064_20230914
66: Image LANDSAT/LC08/C02/T1_L2/LC08_114064_20230930
67: Image LANDSAT/LC08/C02/T1_L2/LC08_114064_20231016
68: Image LANDSAT/LC08/C02/T1_L2/LC08_114064_20231101
69: Image LANDSAT/LC08/C02/T1_L2/LC08_114064_20231117

Koleksi citra untuk melihat suhu permukaan lahan.

Tahun 2015:

0: Image LANDSAT/LC08/C02/T1_L2/LC08_113064_20150410 (ST_B10)
1: Image LANDSAT/LC08/C02/T1_L2/LC08_113064_20150426 (ST_B10)
2: Image LANDSAT/LC08/C02/T1_L2/LC08_113064_20150512 (ST_B10)
3: Image LANDSAT/LC08/C02/T1_L2/LC08_113064_20150613 (ST_B10)
4: Image LANDSAT/LC08/C02/T1_L2/LC08_113064_20150629 (ST_B10)
5: Image LANDSAT/LC08/C02/T1_L2/LC08_113064_20150715 (ST_B10)
6: Image LANDSAT/LC08/C02/T1_L2/LC08_113064_20150917 (ST_B10)
7: Image LANDSAT/LC08/C02/T1_L2/LC08_113064_20151003 (ST_B10)
8: Image LANDSAT/LC08/C02/T1_L2/LC08_114063_20150111 (ST_B10)
9: Image LANDSAT/LC08/C02/T1_L2/LC08_114063_20150127 (ST_B10)
10: Image LANDSAT/LC08/C02/T1_L2/LC08_114063_20150212 (ST_B10)
11: Image LANDSAT/LC08/C02/T1_L2/LC08_114063_20150228 (ST_B10)
12: Image LANDSAT/LC08/C02/T1_L2/LC08_114063_20150316 (ST_B10)
13: Image LANDSAT/LC08/C02/T1_L2/LC08_114063_20150401 (ST_B10)
14: Image LANDSAT/LC08/C02/T1_L2/LC08_114063_20150417 (ST_B10)
15: Image LANDSAT/LC08/C02/T1_L2/LC08_114063_20150503 (ST_B10)
16: Image LANDSAT/LC08/C02/T1_L2/LC08_114063_20150519 (ST_B10)
17: Image LANDSAT/LC08/C02/T1_L2/LC08_114063_20150604 (ST_B10)
18: Image LANDSAT/LC08/C02/T1_L2/LC08_114063_20150620 (ST_B10)
19: Image LANDSAT/LC08/C02/T1_L2/LC08_114063_20150706 (ST_B10)
20: Image LANDSAT/LC08/C02/T1_L2/LC08_114063_20150722 (ST_B10)
21: Image LANDSAT/LC08/C02/T1_L2/LC08_114063_20150807 (ST_B10)
22: Image LANDSAT/LC08/C02/T1_L2/LC08_114063_20150823 (ST_B10)
23: Image LANDSAT/LC08/C02/T1_L2/LC08_114063_20150908 (ST_B10)
24: Image LANDSAT/LC08/C02/T1_L2/LC08_114063_20150924 (ST_B10)
25: Image LANDSAT/LC08/C02/T1_L2/LC08_114063_20151010 (ST_B10)
26: Image LANDSAT/LC08/C02/T1_L2/LC08_114063_20151026 (ST_B10)
27: Image LANDSAT/LC08/C02/T1_L2/LC08_114063_20151111 (ST_B10)
28: Image LANDSAT/LC08/C02/T1_L2/LC08_114063_20151127 (ST_B10)
29: Image LANDSAT/LC08/C02/T1_L2/LC08_114063_20151213 (ST_B10)

30: Image LANDSAT/LC08/C02/T1_L2/LC08_114063_20151229 (ST_B10)
31: Image LANDSAT/LC08/C02/T1_L2/LC08_114064_20150111 (ST_B10)
32: Image LANDSAT/LC08/C02/T1_L2/LC08_114064_20150127 (ST_B10)
33: Image LANDSAT/LC08/C02/T1_L2/LC08_114064_20150212 (ST_B10)
34: Image LANDSAT/LC08/C02/T1_L2/LC08_114064_20150228 (ST_B10)
35: Image LANDSAT/LC08/C02/T1_L2/LC08_114064_20150316 (ST_B10)
36: Image LANDSAT/LC08/C02/T1_L2/LC08_114064_20150401 (ST_B10)
37: Image LANDSAT/LC08/C02/T1_L2/LC08_114064_20150503 (ST_B10)
38: Image LANDSAT/LC08/C02/T1_L2/LC08_114064_20150519 (ST_B10)
39: Image LANDSAT/LC08/C02/T1_L2/LC08_114064_20150604 (ST_B10)
40: Image LANDSAT/LC08/C02/T1_L2/LC08_114064_20150620 (ST_B10)
41: Image LANDSAT/LC08/C02/T1_L2/LC08_114064_20150706 (ST_B10)
42: Image LANDSAT/LC08/C02/T1_L2/LC08_114064_20150722 (ST_B10)
43: Image LANDSAT/LC08/C02/T1_L2/LC08_114064_20150807 (ST_B10)
44: Image LANDSAT/LC08/C02/T1_L2/LC08_114064_20150823 (ST_B10)
45: Image LANDSAT/LC08/C02/T1_L2/LC08_114064_20150908 (ST_B10)
46: Image LANDSAT/LC08/C02/T1_L2/LC08_114064_20150924 (ST_B10)
47: Image LANDSAT/LC08/C02/T1_L2/LC08_114064_20151010 (ST_B10)
48: Image LANDSAT/LC08/C02/T1_L2/LC08_114064_20151026 (ST_B10)
49: Image LANDSAT/LC08/C02/T1_L2/LC08_114064_20151111 (ST_B10)
50: Image LANDSAT/LC08/C02/T1_L2/LC08_114064_20151127 (ST_B10)
51: Image LANDSAT/LC08/C02/T1_L2/LC08_114064_20151213 (ST_B10)
52: Image LANDSAT/LC08/C02/T1_L2/LC08_114064_20151229 (ST_B10)

Tahun 2023:

0: Image LANDSAT/LC08/C02/T1_L2/LC08_113064_20220803 (ST_B10)

1: Image LANDSAT/LC08/C02/T1_L2/LC08_113064_20220819 (ST_B10)

2: Image LANDSAT/LC08/C02/T1_L2/LC08_113064_20220904 (ST_B10)

3: Image LANDSAT/LC08/C02/T1_L2/LC08_113064_20220920 (ST_B10)

4: Image LANDSAT/LC08/C02/T1_L2/LC08_113064_20221006 (ST_B10)

5: Image LANDSAT/LC08/C02/T1_L2/LC08_113064_20221022 (ST_B10)

6: Image LANDSAT/LC08/C02/T1_L2/LC08_113064_20221209 (ST_B10)

7: Image LANDSAT/LC08/C02/T1_L2/LC08_113064_20230126 (ST_B10)

8: Image LANDSAT/LC08/C02/T1_L2/LC08_113064_20230211 (ST_B10)

9: Image LANDSAT/LC08/C02/T1_L2/LC08_113064_20230502 (ST_B10)

10: Image LANDSAT/LC08/C02/T1_L2/LC08_113064_20230518 (ST_B10)

11: Image LANDSAT/LC08/C02/T1_L2/LC08_113064_20230705 (ST_B10)

12: Image LANDSAT/LC08/C02/T1_L2/LC08_113064_20230806 (ST_B10)

13: Image LANDSAT/LC08/C02/T1_L2/LC08_113064_20230822 (ST_B10)

14: Image LANDSAT/LC08/C02/T1_L2/LC08_114063_20220810 (ST_B10)

15: Image LANDSAT/LC08/C02/T1_L2/LC08_114063_20220826 (ST_B10)

16: Image LANDSAT/LC08/C02/T1_L2/LC08_114063_20220911 (ST_B10)

17: Image LANDSAT/LC08/C02/T1_L2/LC08_114063_20220927 (ST_B10)

18: Image LANDSAT/LC08/C02/T1_L2/LC08_114063_20221013 (ST_B10)

19: Image LANDSAT/LC08/C02/T1_L2/LC08_114063_20221029 (ST_B10)

20: Image LANDSAT/LC08/C02/T1_L2/LC08_114063_20221114 (ST_B10)

21: Image LANDSAT/LC08/C02/T1_L2/LC08_114063_20221130 (ST_B10)

22: Image LANDSAT/LC08/C02/T1_L2/LC08_114063_20221216 (ST_B10)

23: Image LANDSAT/LC08/C02/T1_L2/LC08_114063_20230101 (ST_B10)

24: Image LANDSAT/LC08/C02/T1_L2/LC08_114063_20230117 (ST_B10)

25: Image LANDSAT/LC08/C02/T1_L2/LC08_114063_20230202 (ST_B10)

26: Image LANDSAT/LC08/C02/T1_L2/LC08_114063_20230306 (ST_B10)

27: Image LANDSAT/LC08/C02/T1_L2/LC08_114063_20230322 (ST_B10)

28: Image LANDSAT/LC08/C02/T1_L2/LC08_114063_20230407 (ST_B10)

29: Image LANDSAT/LC08/C02/T1_L2/LC08_114063_20230525 (ST_B10)

30: Image LANDSAT/LC08/C02/T1_L2/LC08_114063_20230610 (ST_B10)

31: Image LANDSAT/LC08/C02/T1_L2/LC08_114063_20230626 (ST_B10)

32: Image LANDSAT/LC08/C02/T1_L2/LC08_114063_20230712 (ST_B10)

33: Image LANDSAT/LC08/C02/T1_L2/LC08_114063_20230728 (ST_B10)

34: Image LANDSAT/LC08/C02/T1_L2/LC08_114063_20230813 (ST_B10)

35: Image LANDSAT/LC08/C02/T1_L2/LC08_114063_20230829 (ST_B10)

36: Image LANDSAT/LC08/C02/T1_L2/LC08_114064_20220810 (ST_B10)

37: Image LANDSAT/LC08/C02/T1_L2/LC08_114064_20220826 (ST_B10)

38: Image LANDSAT/LC08/C02/T1_L2/LC08_114064_20220911 (ST_B10)

39: Image LANDSAT/LC08/C02/T1_L2/LC08_114064_20220927 (ST_B10)

40: Image LANDSAT/LC08/C02/T1_L2/LC08_114064_20221013 (ST_B10)

41: Image LANDSAT/LC08/C02/T1_L2/LC08_114064_20221029 (ST_B10)

42: Image LANDSAT/LC08/C02/T1_L2/LC08_114064_20221114 (ST_B10)

43: Image LANDSAT/LC08/C02/T1_L2/LC08_114064_20221130 (ST_B10)

44: Image LANDSAT/LC08/C02/T1_L2/LC08_114064_20230101 (ST_B10)

45: Image LANDSAT/LC08/C02/T1_L2/LC08_114064_20230117 (ST_B10)

46: Image LANDSAT/LC08/C02/T1_L2/LC08_114064_20230322 (ST_B10)

47: Image LANDSAT/LC08/C02/T1_L2/LC08_114064_20230407 (ST_B10)

48: Image LANDSAT/LC08/C02/T1_L2/LC08_114064_20230509 (ST_B10)

49: Image LANDSAT/LC08/C02/T1_L2/LC08_114064_20230525 (ST_B10)

50: Image LANDSAT/LC08/C02/T1_L2/LC08_114064_20230610 (ST_B10)

51: Image LANDSAT/LC08/C02/T1_L2/LC08_114064_20230626 (ST_B10)

52: Image LANDSAT/LC08/C02/T1_L2/LC08_114064_20230712 (ST_B10)

53: Image LANDSAT/LC08/C02/T1_L2/LC08_114064_20230728 (ST_B10)

54: Image LANDSAT/LC08/C02/T1_L2/LC08_114064_20230813 (ST_B10)

55: Image LANDSAT/LC08/C02/T1_L2/LC08_114064_20230829 (ST_B10)

Lampiran 6. *Code Script* Google Earth Engine klasifikasi penutupan lahan tahun 2015 dan tahun 2023

Source Script: (Akram Sri Pandan Buana, 2023) dan Modifikasi Oleh Alif Fitrah.

```
//Klasifikasi Penutupan Lahan Menggunakan Citra Landsat 8 Dengan Algoritma Random Forest Tahun 2015.

Map.centerObject(batas,10);

//Menambahkan fungsi Cloud Masking

function maskL8sr(col) {

  // Bits 3 and 5 are cloud shadow and cloud, respectively.

  var cloudShadowBitMask = (1 << 3);

  var cloudsBitMask = (1 << 5);

  // Mengambil QA Pixel Landsat 8

  var qa = col.select('QA_PIXEL');

  // Both flags should be set to zero, indicating clear conditions.

  var mask = qa.bitwiseAnd(cloudShadowBitMask).eq(0)

                 .and(qa.bitwiseAnd(cloudsBitMask).eq(0));

  return col.updateMask(mask);

}

// Mengaplikasikan Scaling Factor

function applyScaleFactors(image) {

  var opticalBands = image.select('SR_B.').multiply(0.0000275).add(-0.2);

  var thermalBands = image.select('ST_B.*').multiply(0.00341802).add(149.0);

  return image.addBands(opticalBands, null, true)
```

```
            .addBands(thermalBands, null, true);}
// Membuat Kombinasi Band
var vizParams = {
  bands: ['SR_B4', 'SR_B3', 'SR_B2'],
  min: 0,
  max: 0.3,
  gamma: 1.4,
};
var vizParams2 = {
  bands: ['SR_B5', 'SR_B4', 'SR_B3'],
  min: 0,
  max: 0.3,
  gamma: 1.4,
};
var vizParams3 = {
  bands: ['SR_B5', 'SR_B4', 'SR_B3'],
  min: 0,
  max: 0.3,
  gamma: 1.4,
};
var vizParams4 = {
  bands: ['SR_B6', 'SR_B5', 'SR_B4'],
```

```
  min: 0,
  max: 0.3,
  gamma: 1.4,
};
var vizParams5 = {
  bands: ['SR_B6', 'SR_B5', 'SR_B2'],
  min: 0,
  max: 0.3,
  gamma: 1.4,
};
var vizParams6 = {
  bands: ['SR_B7', 'SR_B6', 'SR_B4'],
  min: 0,
  max: 0.3,
  gamma: 1.4,
};
//Mengambil data Citra Landsat 8 Collection 2 SR
var col= ee.ImageCollection('LANDSAT/LC08/C02/T1_L2')
    .map(maskL8sr).map(applyScaleFactors)
    .filterDate('2015-01-01','2015-12-31')
    .filterBounds(batas)
    .map(function(image){return image.clip(batas)});
```

```
print('collecion',col);

//reduksi koleksi citra tahun pemantauan

var image = col.median();

        // .select(['SR_B4','SR_B3','SR_B2']);

//print('image', image);

// Menambahkan Kombinasi Band Ke Layer

Map.addLayer(image, vizParams, '432 Natural');

// Map.addLayer(image, vizParams2, '543 Vegetation Infrared');

// Map.addLayer(image, vizParams3, '564 Land/Water');

// Map.addLayer(image, vizParams4, '654 Vegetation Analysis');

// Map.addLayer(image, vizParams5, '652 Agriculture');

// Map.addLayer(image, vizParams6, '764 Urban');

//Membuat training data

var aoi = Vegetasi.merge(Badan_Air).merge(Lahan_Terbangun)

.merge(Tambak).merge(Lahan_Terbuka).merge(Sawah);

var bands = ['SR_B1','SR_B2', 'SR_B3', 'SR_B4', 'SR_B5', 'SR_B6', 'SR_B7'];

var trainingset = image.select(bands).sampleRegions({

collection: aoi,

properties: ['LC'],

scale: 30

});

print(trainingset);
```

```
//Membuat Klasifikasi Penutupan Lahan dengan Algoritma Random Forest
var classifier = ee.Classifier.smileRandomForest(6).train({
features: trainingset,
classProperty: 'LC',
inputProperties: bands
});
//Menjalankan Klasifikasi
var classified = image.select(bands).classify(classifier);
//Menampilkan Hasil Kalasifikasi Penutupan Lahan
Map.addLayer(classified,
{min: 0, max: 6,
palette:['#00d402','#1488ff','#ff0f0f','#00ffff','#e8c8ff','#7987ff','#fff991']},
'RF2015');
//Menyimpan hasil klasifikasi ke google drive
Export.image.toDrive({
  image: classified,
  description: 'PL_RF_2023_Sinjai',
  region: batas,
  scale: 30,
  maxPixels: 1e9,
});
// Export Training Sample
```

```
Export.table.toDrive({
  collection :Lahan_Terbangun,
  description : 'lahanterbangun',
  fileFormat : 'shp',
  });
//Klasifikasi Penutupan Lahan Menggunakan Citra Landsat 8 Dengan Algoritma Random Forest Tahun 2023
Map.centerObject(batas,10);
//Menambahkan fungsi Cloud Masking
function maskL8sr(col) {
  // Bits 3 and 5 are cloud shadow and cloud, respectively.
  var cloudShadowBitMask = (1 << 3);
  var cloudsBitMask = (1 << 5);
  // Mengambil QA Pixel Landsat 8
  var qa = col.select('QA_PIXEL');
  // Both flags should be set to zero, indicating clear conditions.
  var mask = qa.bitwiseAnd(cloudShadowBitMask).eq(0)
                 .and(qa.bitwiseAnd(cloudsBitMask).eq(0));
  return col.updateMask(mask);
}
// Mengaplikasikan Scaling Factor
function applyScaleFactors(image) {
```

```
  var opticalBands = image.select('SR_B.').multiply(0.0000275).add(-0.2);
  var thermalBands = image.select('ST_B.*').multiply(0.00341802).add(149.0);
  return image.addBands(opticalBands, null, true)
              .addBands(thermalBands, null, true);}
// Membuat Kombinasi Band
var vizParams = {
  bands: ['SR_B4', 'SR_B3', 'SR_B2'],
  min: 0,
  max: 0.3,
  gamma: 1.4,
};
var vizParams2 = {
  bands: ['SR_B5', 'SR_B4', 'SR_B3'],
  min: 0,
  max: 0.3,
  gamma: 1.4,
};
var vizParams3 = {
  bands: ['SR_B5', 'SR_B4', 'SR_B3'],
  min: 0,
  max: 0.3,
  gamma: 1.4,
```

```
};
var vizParams4 = {
  bands: ['SR_B6', 'SR_B5', 'SR_B4'],
  min: 0,
  max: 0.3,
  gamma: 1.4,
};
var vizParams5 = {
  bands: ['SR_B6', 'SR_B5', 'SR_B2'],
  min: 0,
  max: 0.3,
  gamma: 1.4,
};
var vizParams6 = {
  bands: ['SR_B7', 'SR_B6', 'SR_B4'],
  min: 0,
  max: 0.3,
  gamma: 1.4,
};
//Mengambil data Citra Landsat 8 Collection 2 SR
var col= ee.ImageCollection('LANDSAT/LC08/C02/T1_L2')
    .map(maskL8sr).map(applyScaleFactors)
```

```
    .filterDate('2023-01-01','2023-12-31')
    .filterBounds(batas)
    .map(function(image){return image.clip(batas)});
print('collecion',col);
//reduksi koleksi citra tahun pemantauan
var image = col.median();
            // .select(['SR_B4','SR_B3','SR_B2']);
//print('image', image);
// Menambahkan Kombinasi Band Ke Layer
Map.addLayer(image, vizParams, '432 Natural');
// Map.addLayer(image, vizParams2, '543 Vegetation Infrared');
// Map.addLayer(image, vizParams3, '564 Land/Water');
// Map.addLayer(image, vizParams4, '654 Vegetation Analysis');
// Map.addLayer(image, vizParams5, '652 Agriculture');
// Map.addLayer(image, vizParams6, '764 Urban');
// // Export Citra To Drive
// Export.image.toDrive({
//   image: image,
//   description: 'L8_2023_SNJ',
//   region: batas,
//   scale: 30,
//   maxPixels: 1e9,
```

```
// });
//Membuat training data
var aoi = Vegetasi.merge(Badan_Air).merge(Lahan_Terbangun)
.merge(Tambak).merge(Lahan_Terbuka).merge(Sawah_Basah).merge(Sawah_Ke
ring);
var bands = ['SR_B1','SR_B2', 'SR_B3', 'SR_B4', 'SR_B5', 'SR_B6', 'SR_B7'];
//
var trainingset = image.select(bands).sampleRegions({
collection: aoi,
properties: ['LC'],
scale: 30
});
print(trainingset);
//Membuat Klasifikasi Penutupan Lahan dengan Algoritma Random Forest
var classifier = ee.Classifier.smileRandomForest(6).train({
features: trainingset,
classProperty: 'LC',
inputProperties: bands
});
//Menjalankan Klasifikasi
var classified = image.select(bands).classify(classifier);
//Menampilkan Hasil Kalasifikasi Penutupan Lahan
```

```
Map.addLayer(classified,
{min: 0, max: 6,
palette:['#00d402','#1488ff','#ff0f0f','#00ffff','#e8c8ff','#7987ff','#fff991']},
'RF2023');
//Menyimpan hasil klasifikasi ke google drive
Export.image.toDrive({
  image: classified,
  description: 'PL_RF_2023_Sinjai',
  region: batas,
  scale: 30,
  maxPixels: 1e9,
});
// Export Training Sample
Export.table.toDrive({
  collection :Lahan_Terbangun,
  description : 'lahanterbangun',
  fileFormat : 'shp',
  });
```

Lampiran 7. Code Script Google Earth Engine perhitungan suhu permukaan lahan Kabupaten Sinjai tahun 2015 dan tahun 2023

Source Script: (Almustafa Ayek, Alif Fitrah, dan Akram Sri Pandan Buana, 2023).

```
//Perhitungan Suhu Permukaan Lahan Dengan Landsat 8 Kabupaten Sinjai Tahun 2015

Map.centerObject(roi)

//Mengaplikasikan masking dan scale factor

function maskL89sr(image) {

  var qaMask = image.select('QA_PIXEL').bitwiseAnd(parseInt('11111', 2)).eq(0);

  var saturationMask = image.select('QA_RADSAT').eq(0);

//Konversi DN Ke Surface Reflectance

  var opticalBands = image.select('SR_B.').multiply(0.0000275).add(-0.2);

//Konversi DN Band Thermal Ke LST dalam derajat Celcius

  var thermalBands = image.select('ST_B.*').multiply(0.00341802).add(149.0).add(-273.15);

  return image.addBands(opticalBands, null, true)

      .addBands(thermalBands, null, true)

      .updateMask(qaMask)

      .updateMask(saturationMask);

}

var vizParams2 = {

  bands: ['SR_B4', 'SR_B3', 'SR_B2'],

  min: 0,

  max: 0.3,

  gamma: 1.4,

};

//Memnaggil data Landsat 8
```

```
var landsat = ee.ImageCollection('LANDSAT/LC08/C02/T1_L2')
    .filterDate('2015-01-01', '2015-12-31')
    .map(maskL89sr)
    .filterBounds(roi)
    .map(function(image){return image.clip(roi)})
  ;
    print(landsat)
var image = landsat  .mean();
Map.addLayer(image,vizParams2, 'Landsat')
//Mengambil data band thermal Landsat 8
var LST =image.select('ST_B10');
//Memotong data citra dengan region of interest
var LST= LST.clip(roi);
//Memvisualisasikan data LST
var landSurfaceTemperatureVis = {
  min: 0,
  max: 40,
  palette: [
    '040274', '040281', '0502a3', '0502b8', '0502ce', '0502e6',
    '0602ff', '235cb1', '307ef3', '269db1', '30c8e2', '32d3ef',
    '3be285', '3ff38f', '86e26f', '3ae237', 'b5e22e', 'd6e21f',
    'fff705', 'ffd611', 'ffb613', 'ff8b13', 'ff6e08', 'ff500d',
    'ff0000', 'de0101', 'c21301', 'a71001', '911003'
  ],
};
//Memunculkan data LST di Layer
```

```
Map.addLayer(
    LST, landSurfaceTemperatureVis,
    'Land Surface Temperature');
//Mengekspor data ke Google Drive dalam bentuk raster
Export.image.toDrive({
  image: LST,
  description: 'LST',
  scale: 30,
  region: roi,
  fileFormat: 'GeoTIFF',
});
//Perhitungan Suhu Permukaan Lahan Dengan Landsat 8 Kabupaten Sinjai Tahun 2023
Map.centerObject(roi);
//Mengaplikasikan masking dan scale factor
function maskL89sr(image) {
  var qaMask = image.select('QA_PIXEL').bitwiseAnd(parseInt('11111', 2)).eq(0);
  var saturationMask = image.select('QA_RADSAT').eq(0);
//Konversi DN Ke Surface Reflectance
  var opticalBands = image.select('SR_B.').multiply(0.0000275).add(-0.2);
//Konversi DN Band Thermal Ke LST dalam derajat Celcius
  var thermalBands = image.select('ST_B.*').multiply(0.00341802).add(149.0).add(-273.15);
  return image.addBands(opticalBands, null, true)
```

```
      .addBands(thermalBands, null, true)
      .updateMask(qaMask)
      .updateMask(saturationMask);
}
var vizParams2 = {
  bands: ['SR_B4', 'SR_B3', 'SR_B2'],
  min: 0,
  max: 0.3,
  gamma: 1.4,
};
//Memnaggil data Landsat 8
var landsat = ee.ImageCollection('LANDSAT/LC08/C02/T1_L2')
    .filterDate('2022-08-01', '2023-08-31')
    .map(maskL89sr)
    .filterBounds(roi)
    .map(function(image){return image.clip(roi)})
  ;
    print(landsat);
var image = landsat  .mean();
Map.addLayer(image,vizParams2, 'Landsat');
//Mengambil data band thermal Landsat 8
var LST =image.select('ST_B10');
```

```
//Memotong data citra dengan region of interest
var LST= LST.clip(roi);
//Memvisualisasikan data LST
var landSurfaceTemperatureVis = {
  min: 0,
  max: 40,
  palette: [
    '040274', '040281', '0502a3', '0502b8', '0502ce', '0502e6',
    '0602ff', '235cb1', '307ef3', '269db1', '30c8e2', '32d3ef',
    '3be285', '3ff38f', '86e26f', '3ae237', 'b5e22e', 'd6e21f',
    'fff705', 'ffd611', 'ffb613', 'ff8b13', 'ff6e08', 'ff500d',
    'ff0000', 'de0101', 'c21301', 'a71001', '911003'
  ],
};
//Memunculkan data LST di Layer
Map.addLayer(
    LST, landSurfaceTemperatureVis,
    'Land Surface Temperature');
//Mengekspor data ke Google Drive dalam bentuk raster
Export.image.toDrive({
  image: LST,
  description: 'LST',
```

```
  scale: 30,
  region: roi,
  fileFormat: 'GeoTIFF',
});
```